Chapter-4

Experimentation

4.1 Introduction:

There are several techniques available in the literature for the synthesis of ceramic samples. There are mainly two approaches for synthesis. One is the chemical method and the other is the mechanical method. Mechanical methods are mainly of two type (a) mixed oxide process or solid state reaction process and (b) high energy ball milling. Similarly, for the synthesis of the ceramics powder commonly used chemical methods are (a) sol-gel methods, (b) co-precipitation method, (c) hydrothermal method (d) combustion method etc. Both the chemical and mechanical methods have their own advantages and disadvantages. The mechanical method is successful for a large-scale production of bulk ceramic powders at its low cost and easy adaptability. In conventional solid-state method, high temperature and heating for prolonged time makes the particles coarse. Fine powders mainly prepared by chemical process have an improved homogeneity, densifications and the chemical precursors used in this process can easily be refined to increase the purity. However, in many cases, the chemical routes generally involve complex techniques when compared to the conventional solid state methods. In the present study CCTO ceramics were prepared by the most economical mixed oxide process i.e., high temperature solid state reaction technique.

4.2 The Oxide Route Method for Preparing CCTO:

$CaCu_3Ti_4O_{12}$ (CCTO) polycrystalline ceramics were prepared by solid-state reaction. The materials used for preparing CCTO ceramic powder were as follows:

1) CuO (Copper Oxide, ≥99.90%)
2) CaO (Calcium Oxide, ≥99.95%
3) TiO_2 (Titanium Oxide, ≥99.7%)

All the above materials mentioned in the list were procured from Sigma Aldrich.

These materials were ball milled in a mill lined with rubber and containing zirconia balls. The ball milling has been carried out for at least 24 hours with acetone as the dispersant. The ball milled powder is then sieved using a 5 μm mesh. The sieved powder has been compacted lightly in a crucible made of high grade alumina. Since the particle size of the constituent oxides plays a major part in the physical properties of the ceramic, therefore sieved powder was again sieved before compaction and sintering. The mixed powders were then poured in a crucible and calcined in an electrical temperature-controlled furnace, strictly following the steps mentioned below:

Step 1: Starting from room temperature, the temperature of the furnace is raised to 500 °C in 3 hours at an even rate; it is then kept constant at 500 °C for 2 hours;

Step 2: The furnace temperature is then raised to 850 °C in 2 hours at an even rate. It is then maintained at a constant temperature of 850 °C for an hour;

Step 3: at last the furnace temperature is raised to 1100 °C from 850 °C in 2 hours at an even pace. It is then kept constant at 1100°C for 2 hours.

The reason for keeping temperatures constant for a few hours at 500 °C, 850 °C is so that any water and alcohol that may still exist in the material will vaporize at these 2 temperatures, while 1100°C is the definite temperature at which the solid state reaction starts. The calcined powders were firstly milled and then sieved. They were pressed into pellets in a cylinder shape of appropriate thickness. The pellets were then put in a high-temperature furnace to be sintered, with the increases in temperature following these 3 steps; first two steps are exactly the with the calcining part; Step 3: Raise to 1250 °C from 850 °C in 3 hours evenly, and then keep constant at 1250 °C for 12 hours. The sintered pellet samples were first polished into a smooth cylinder. Thickness and diameter were then measured using a vernier caliper with an accuracy of 0.05mm. Density obtained based on these measurements will be used when comparing with the theoretical density. Figure 4.1. shows a flowchart of the mixed oxide route for making CCTO ceramics. The first step in characterization

of the sample starts with evaluating the density of the samples by Archimedes principle.

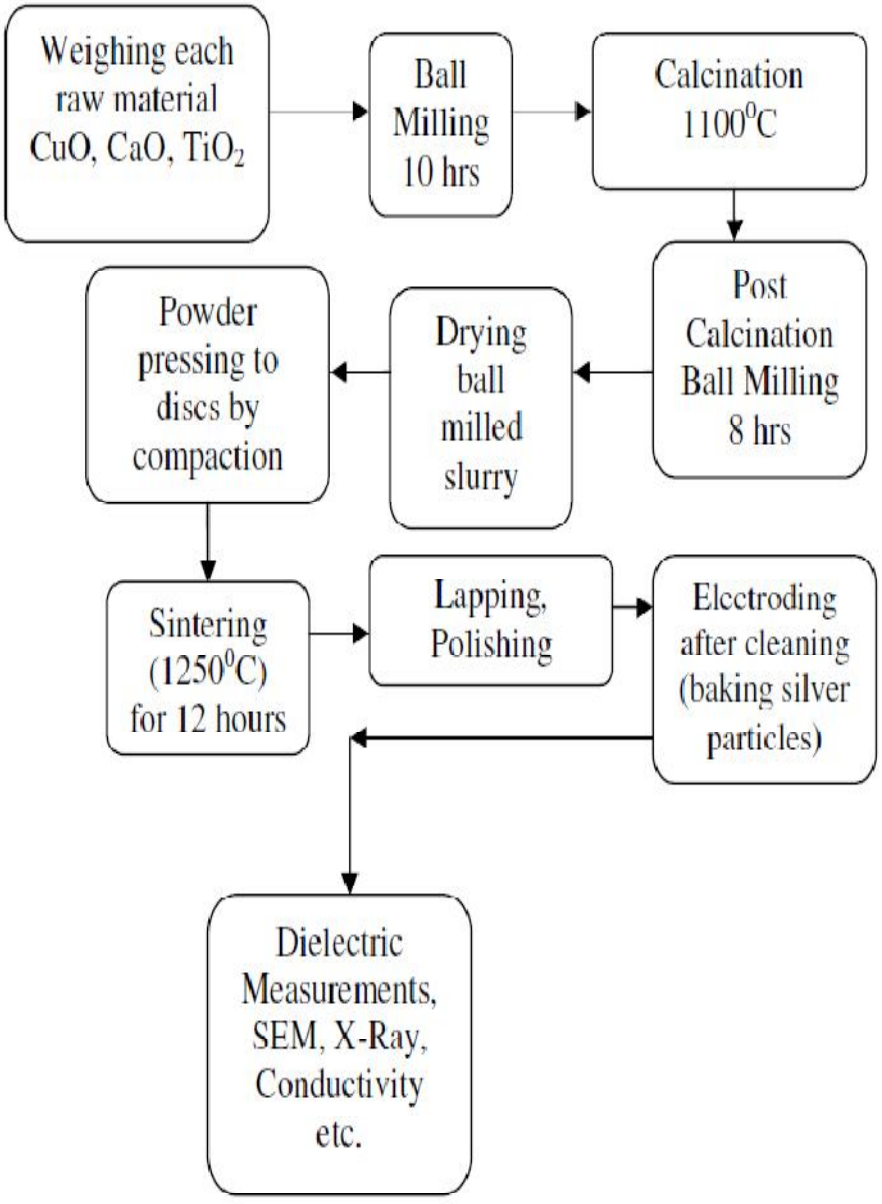

Figure-4.1: The mixed oxide route of CCTO ceramic preparation

4.3 Preparation of the CCTO-PVC Composites:

The materials used for preparing the composites were as follows:

3) CCTO powders prepared in the lab as mentioned in previous section.
4) Poly Vinyl Chloride (PVC) and Polyethylene terephthalate (PET).

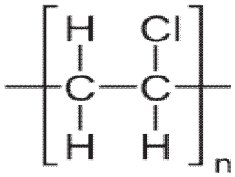

PVC

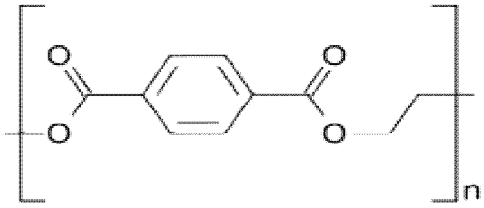

PET

CCTO: PVC composites of 0-3 connectivity was prepared by mixing pre sintered powder of CCTO ceramic which was prepared according to the method mentioned in section above and PVC and PET procured from Sigma Aldrich. The density of CCTO powder (4.93 gm/cc) was elucidated using standard techniques. The first set of samples were prepared in such a way that the material contains ninety percent (90%) by volume of CCTO ceramic and ten percent (10%) by volume of PVC. The calculated amount of the constituents of the composite (CCTO ceramic powder and PVC) were weighed and mixed thoroughly in a mortar and pestle made of Agate, this was to minimize the amount of unwanted impurities getting into the bulk of the

material prepared. Tetrahydrofuran (THF) is used as a solvent so that a paste of the ceramic and PVC is formed, now one assumes that CCTO powder has been evenly got distributed into a matrix of PVC. The paste is now injected into steel dies (moulds) which are designed to withstand high pressures and temperatures, and they are also air tight so that application of pressure spreads uniformly into the bulk of the material injected into it without any material leaking out of the cavity. The mould loaded with the paste is then heated to 80^0-140^oC with the pressure on and the pressure gauge reading 25 tonnes. The temperature was held for 30 minutes after which the heater was put off and the mould was allowed to cool to room temperature with the applied pressure on. After the mould reaches room temperature, and the pressure released, the mould is opened and the material inside the cavity is removed. This is now a 0:3 ceramic polymer composite samples. The cavity of the die was circular with a diameter of 2 inches (50 mm), therefore the shape of the sample is a circular disc, with an appropriate thickness. The thickness of the composite samples can be varied by adjusting the amount of paste being poured into the die. Since the diameter of the composite sample made with the above mentioned die / mould is a constant and therefore it cannot exceed 50 mm, more amount of paste will only result in a thicker composite sample. Calculated amount of paste was loaded into the mould so that the resulting sample yields a thickness not more than 1.5 mm. One can in principle mould the material into any desired shape and size using this procedure. All it needs is a mould with the design features as mentioned and a cavity of the desired shape. In the case of CCTO : PET composites instead of THF the solvent used was Dichloromethane (DCM) and the rest of the procedures were same as in PVC composites.

In the present work as mentioned before the samples are in the shape of thin discs with thickness not more than 1.5 mm. Some of the samples were coated with silver on its plane sides (faces) using a vacuum coating unit. Care was taken to mask away the silver electrodes from the edges of the samples. That is the silver electrode coated onto the samples had a diameter 2mm less than the diameter of the sample. For conductivity studies electroded and unpoled samples were used. For X-ray analysis it was not electroded while samples chosen for SEM were coated on one side with gold using a sputtering system. Figure 4.2 displays a flow diagram of the

composite preparation. About 10 samples of each composition were prepared. The procedure mentioned above was repeated for samples of composition 90% by

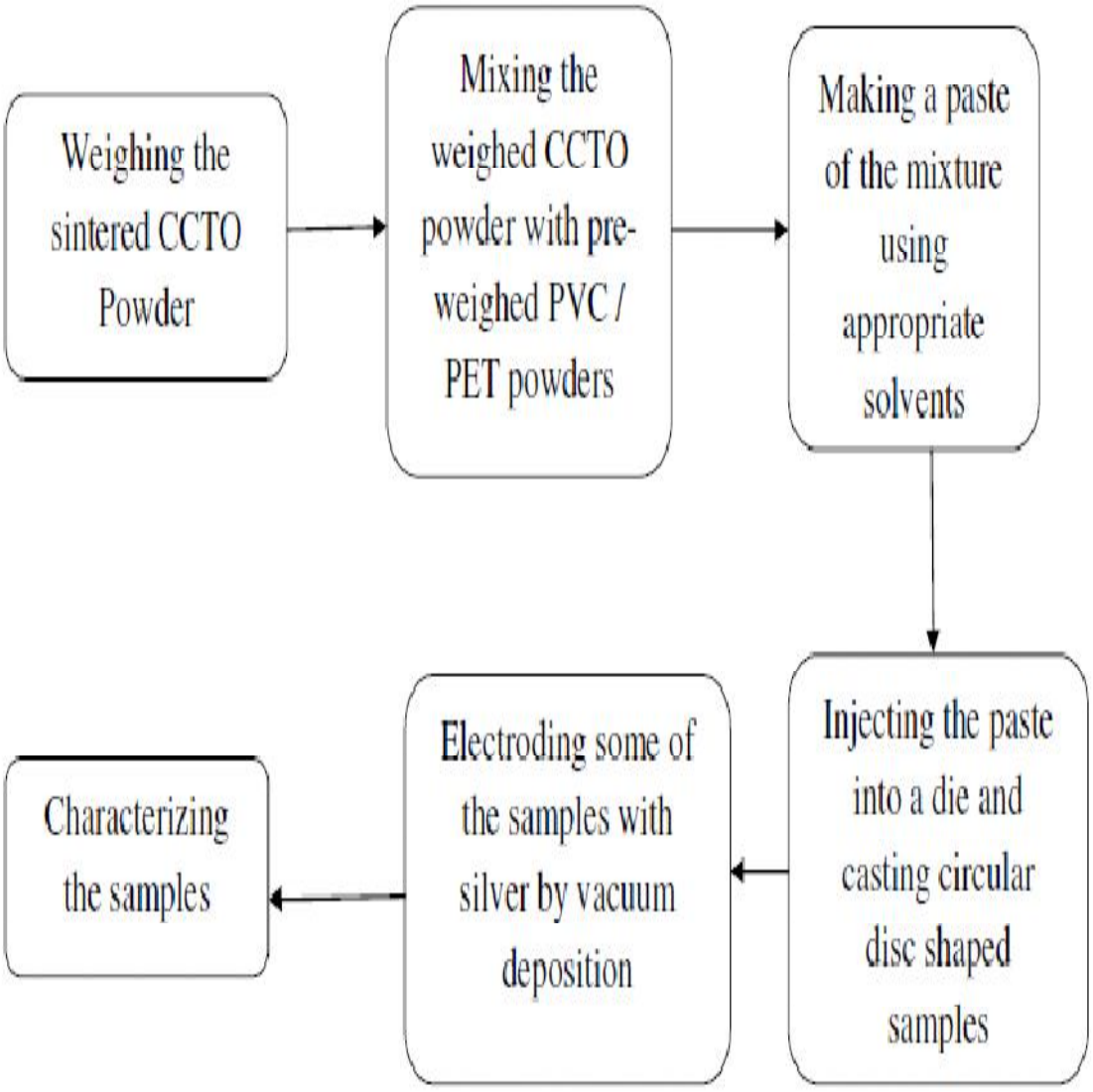

volume CCTO, 80%,70%, 60%, 50%, 40% and 30%.

Fig-4.2: Flow Chart of the Composite Preparation

4.4 Characterization :

4.4.1 X-Ray Characterization:

Many properties of polycrystalline electroceramics fall far below the figures of merit for single crystals. The addition of certain dopants can also strongly influence grain shape and microstructural anisotropy during the sintering stage.

The most common diffraction technique employs a powdered or polycrystalline specimen consisting of many fine and randomly oriented particles that are exposed to monochromatic x-radiation. Each powder particle (or grain) is a crystal, and having a large number of them with random orientations ensures that some particles are properly oriented such that every possible set of crystallographic planes will be available for diffraction. The diffractometer is an apparatus used to determine the angles at which diffraction occurs for powdered specimens; its features are represented schematically in figure 4.3.

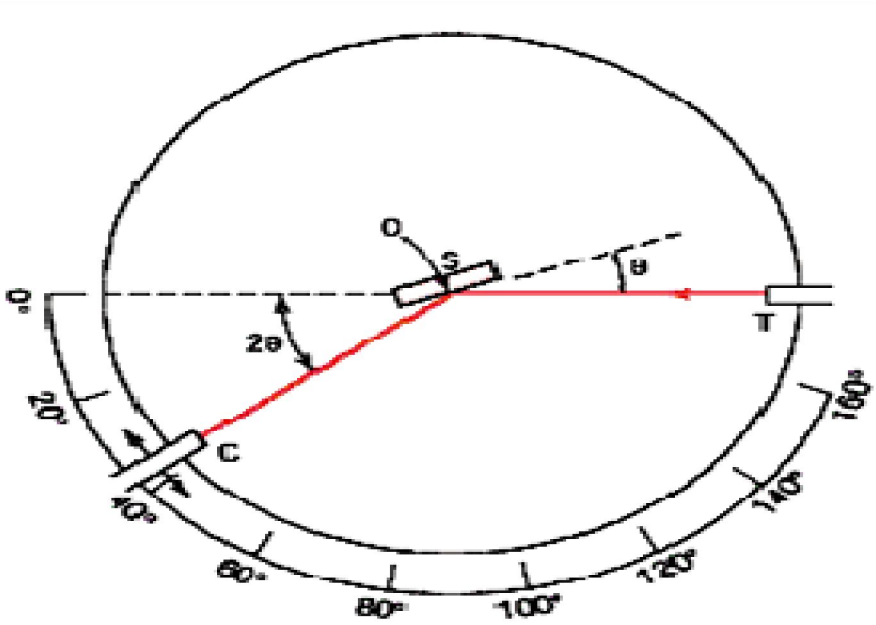

Figure4.3: Schemtaic diagram of an X-ray diffractometer; T is the X-ray source, S the specimen, C the detector and O the axis around which the specimen and detector rotate.

The monochromatic X-ray beam is generated at point T, and the intensities of diffracted beams are detected with a counter labeled C in the figure. The specimen, X-ray source, and counter are all coplanar. The counter is mounted on a movable carriage that may also be rotated about the O axis; its angular position in terms of 2θ is marked on a graduated scale. Carriage and specimen are mechanically coupled such that a rotation of the specimen through θ is accompanied by a 2θ rotation of the counter; this assures that the incident and reflection angles are maintained equal to one another. Collimators are incorporated within the beam path to produce a well-defined and focused beam. Utilization of a filter provides a near-monochromatic beam. As the counter moves at constant angular velocity, a recorder automatically plots the diffracted beam intensity (monitored by the counter) as a function of 2θ; 2θ is termed the diffraction angle, which is measured experimentally. Other powder techniques have been revised wherein diffracted beam intensity and position are recorded on a photographic film instead of being measured by a counter. One of the

primary uses of X-ray diffractometry is for the determination of crystal structure. The unit cell size and geometry may be resolved from the angular positions of the diffraction peaks, whereas arrangement of atoms within the unit cell is associated with the relative intensities of these peaks.

X-rays, as well as electron and neutron beams, are also used in other types of material investigations. For example, crystallographic orientations of single crystals are possible using X-ray diffraction (or Laue) photographs. Other uses of X-rays include qualitative and quantitative chemical identifications, and the determination of residual stresses and crystal size. In the present study the particle size of the CCTO powder dispersed in the composite was also determined using the full width at half maximum of the diffraction peaks and substituting in the Debye Scherer formula.

4.4.2 Scanning Electron Microscope (SEM) :

The scanning electron microscope is used to determine the average crystallite size and the surface morphology [102]. It gives information about the grain evolution and grain size. It also gives the information about the inter-granular and the intra-granular pores and the distribution of grains in the composite samples. SEM measurements are based on the principle of irradiating the specimen with a finely focused electron beam. The secondary electrons, backscattered electrons, auger electrons, characteristic X-rays and several other radiations are released from the specimen. Generally, the secondary electrons are collected to form the image in the SEM mode. The reflected (or back-scattered) beam of electrons are collected, and then displayed at the same scanning rate on a cathode ray tube (similar to a TV screen). The image on the screen, which may be photographed, represents the surface features of the specimen. The surface under study may or may not be polished and etched, but it must be electrically conductive; a very thin metallic surface coating must be applied to nonconductive materials. Magnifications ranging from 10 to in excess of 50,000 diameters are possible, as are also very great depths-of-field. Accessories and equipments permits qualitative and semi quantitative analysis of the elemental composition of much localized surface areas. In the present study the microscope viz. XL30, Philips Co., USA**,** was used for characterization. The instrument was used under high vacuum conditions. Surface viewing consisted of securing the samples

(surface side parallel to the viewing stub) directly to the carbon coated tape. After the sample stubs were mounted, samples were coated with gold (Denton Desk II sputtering system, 40 mA, 30 s). Samples were loaded onto an SEM mount and screwed in the sample holder within the SEM. Vacuum was applied to the instrument and imaging commenced at 10-15 kV and as soon as 1.4×10^{-5} mm Hg pressure was attained in the SEM.

4.4.3 Dielectric Spectroscopy:

Dielectric relaxations in materials occur at various frequencies, depending on the type of chemical or physical defects [103]. These defects depend on either intrinsic or extrinsic heterogeneities due to special heat treatments (quenching, annealing, etc.), ionic substitutions, grain size additives, and grain boundary nature. The value of the relaxation frequency f_r increases from about 10^2 to 10^{12} Hz as the scale of the defect phenomenon decreases from microstructure, to nanostructure, to unit cell, to atomic vibrations. This type of study requires a multidisciplinary approach involving solid state chemistry, materials science, solid state physics and various industrial aspects. The applications in the area of electronic ceramics and composites are related to the value of f_r. In absorbents, the usable frequency is close to f_r, whereas it is far from f_r in good insulators.

In view of numerous experimental examples, a classification is proposed to predict which materials may be suitable for a given application. When an alternating current is applied to a sample, the dipoles responsible for the polarization are no longer able to follow the oscillations of the electric field at certain frequencies. The field reversal and the dipole reorientation become out-of-phase, giving rise to energy dissipation, this effect is called dielectric relaxation and may be evidenced by a drop in ε' and a maximum in the imaginary part of the permittivity, ε'', at the relaxation frequency f_r .The value of f_r may range from low to high frequencies depending on the type of chemical or physical defects related to the dipoles considered. Defects may cause modifications of the short and/or long-range interactions in inorganic ferroelectrics.

More generally, ferroelectric behaviour and dielectric properties are very sensitive to both external (temperature, electric field, ionic substitution, etc.) and intrinsic (defect, domain configuration, etc.) modifications because the polarization is largely affected

[104]. The dielectric spectroscopy requires different methods of measurement according to the frequency range. The science of dielectrics is multidisciplinary encompassing the fields of physics, chemistry and electrical engineering.

Over a wide frequency range, different types of polarization cause several dispersion regions (Figure 4.4). The critical frequency, characteristic of each contributing mechanism, depends on the nature of the dipoles. When the frequency increases, the number of mechanisms involved in the dynamic polarization decreases. At very high frequencies, only the electronic contribution of the polarization remains [105]. A decrease of ε' is observed with increasing frequency. Each polarization mechanism is characterized by a critical frequency f_r (relaxation frequency) corresponding to the maximal phase shift between the polarization P and the applied electric field E; a maximum of dielectric losses (tan δ ~ ε''/ε' is the loss factor) occurs.

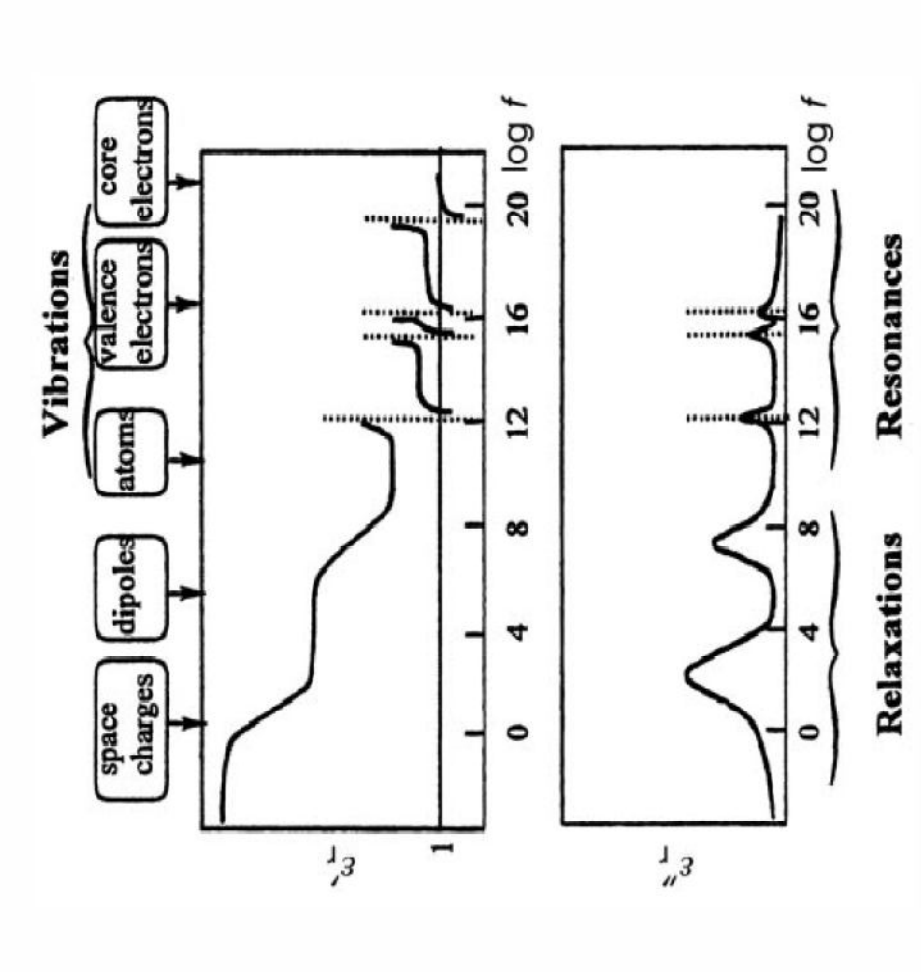

Fig 4.4: Schematic representation of various relaxation processes

The orientation polarizations, i.e. interfacial polarization (space charges) and dipole polarization, are observed from low to microwave frequencies. The force opposed to the motion is here of a frictional nature and the resulting dynamics are thus of the relaxational type. The deformation polarizations, i.e. ionic (oscillations of ions) and electronic polarizations (displacement of electrons with respect to the nuclei), are detected in short microwave and infrared ranges. The latter mechanisms lead to resonance-type dielectric dispersions (vibrational process, harmonic oscillator type). The concept of dipoles giving rise to polarization was introduced by Debye [106]. The Debye model considers the re orientation of non-interacting dipoles in a purely

viscous environment without an elastic restoring force. The expression for the complex permittivity is:

$$\varepsilon^*(\omega) = \varepsilon_\infty + (\varepsilon_S - \varepsilon_\infty)/(1+i\omega\tau) \qquad \text{---------- (4.1)}$$

Separation of the real and imaginary parts of the permittivity gives:

$$\varepsilon' = \varepsilon_\infty + (\varepsilon_S - \varepsilon_\infty)/(1+(\omega\tau)^2)$$

$$\varepsilon'' = (\varepsilon_S - \varepsilon_\infty)/(1+(\omega\tau)^2)\omega\tau$$

---------- (4.2)

Where τ is the relaxation time, ε_S is the permittivity at low frequency (f « relaxation frequency) and ε_∞ the one at high frequency (f » relaxation frequency). ε' decreases to ε_∞ with increasing frequency and ε'' is maximal at the frequency $\omega \sim 1/\tau$ (Fig. 4.5).

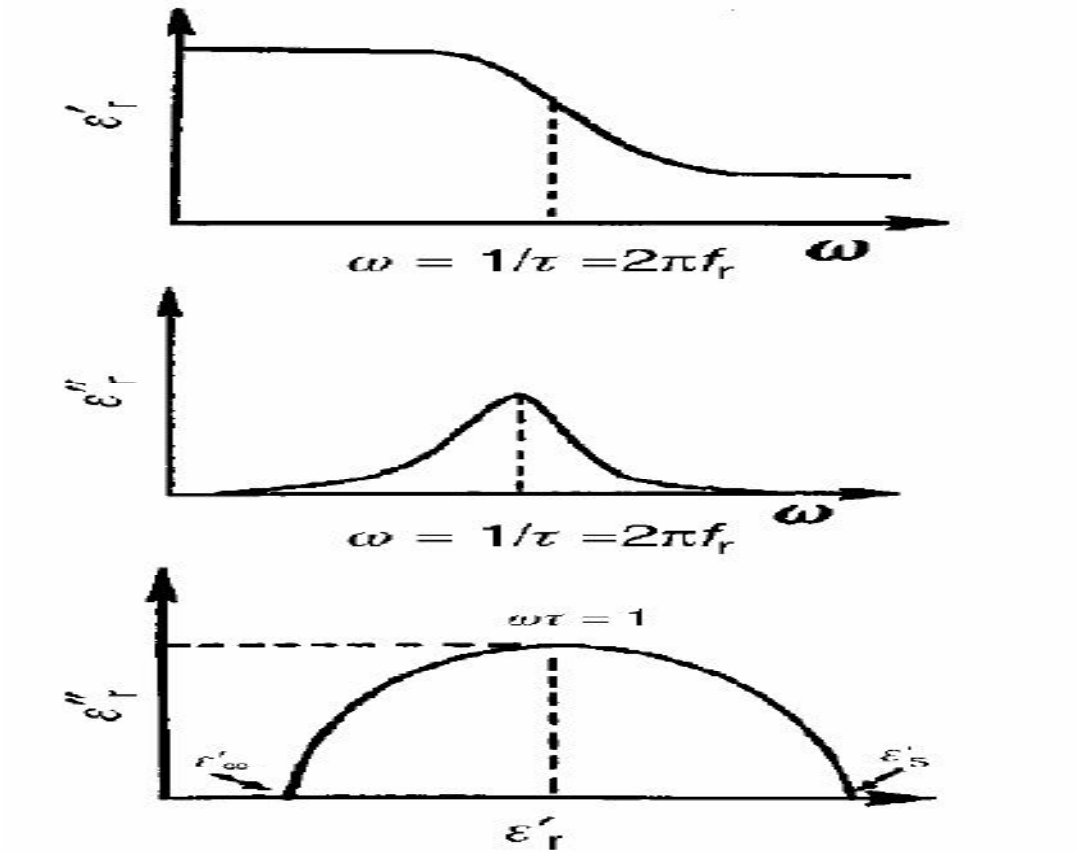

Figure 4.5: Frequency dependence of ε' and ε" and an Argand diagram

Debye Model

In the case of dipoles correlated through ferroelectric-type interactions, it is possible to translate the thermal variation of permittivity at various frequencies (suitable to characterize the transition and given classically) into frequency dielectric dispersion curves at fixed temperatures. Argand diagrams (ε" versus ε') are also sometimes used for relaxation studies instead of the temperature and frequency variations of ε" and ε'. The corresponding curves are of course related to each other (Fig. 4.5). The obtained curve is a semi-circle centered on the abscissa axis at the $(\varepsilon_s - \varepsilon_\infty)/2$, point. Two parameters are characteristic of the Debye relaxation: the relaxation step $\Delta\varepsilon'=\varepsilon_s-\varepsilon_\infty$ and the relaxation time τ. The dielectric dispersion Δε' is then obtained by extrapolating at very low frequency ($f \ll f_r$) for ε_s and at infinite frequency ($f \gg f_r$) for ε_∞. Such parameters are related to the dipole characteristics: Δε' is related to both the microscopic dipolar moment p and the number N of relaxing dipoles through the Langevin relation:

$$\varepsilon_s - \varepsilon_\infty \approx Np^2/3kT \qquad \text{----------(4.3)}$$

k is the Boltzmann constant (k~8.617385 eV K^{-1}).The value of τ is correlated with the energy barrier ΔE separating the two minima corresponding to the two equivalent positions of the non-interacting dipoles in a double-well potential (viscous interaction between the dipole and the environment). The variation of the relaxation time may be expressed as a thermally activated process:

$$\tau = \tau_0 \exp(\Delta E/kT) \qquad \text{---------- (4.4)}$$

$$\varepsilon^*(\omega) = \varepsilon_\infty + (\varepsilon_s - \varepsilon_\infty)/(1+(j\omega\tau)^\alpha) \qquad \text{---------- (4.5)}$$

with $\tau_o \sim 1/\omega_o$, ω_o being an extrapolated attempt frequency. The atoms are oscillating through the equilibrium position at the frequency $\omega_o/2\pi$ and acquire sufficient energy to cross the barrier. In polar dielectrics, corrections to the simple Debye model are often necessary. Cole–Cole plots (Argand diagram, i.e. ε'' versus ε') reflect the deviation from the ideal Debye model and introduce a parameter α which reflects a distribution of the relaxation time. Another example is the presence of conductivity (σ), which leads to an additional term in the Debye equation

$$\varepsilon^*(\omega) = \varepsilon_\infty + (\varepsilon_s - \varepsilon_\infty)/(1+(j\omega\tau)^\alpha) - j\sigma/\omega \quad \text{---------- (4.6)}$$

where j is a complex number. In this latter case, the complex impedance is usually measured. Charge carriers in dielectric materials have to be considered in polarization mechanisms. The electric field can interact in a solid not only through reorientation of the electric dipoles but also through the displacement of the charge carriers. The key point is the degree of localization of these carriers. Mobile or free charges (electrons or holes) lead to a significant contribution only up to 10^{11} Hz. On the contrary, bound charges can be considered as dipoles and participate in polarization. Dissipation can arise from the hopping process in ionic conductivity. The hopping ionic motion through defects is a thermally activated process and its contribution is observed at high temperature. A carrier leading to a local lattice deformation and trapped in the potential well, i.e. a polaron, contributes to the dielectric properties particularly at very low temperature. Space charges (carriers located at the grain boundary in polycrystalline materials) act as dipoles under an ac field and participate in polarization; the corresponding materials are called grain boundary layer dielectrics. All these contributions lie in the frequency range 10 Hz–1M Hz according to the temperature which is a determining parameter in conduction phenomena. The classical model of Debye allows for characterization of the impedance behaviour. The material is then described electrically by a parallel equivalent circuit of pure resistance R and capacitance C. The impedance of this model is $Z^*=R/(j\omega/\omega_1)$, where ω_1 is the characteristic frequency of the circuit, $\omega_1=1/RC$. The response in the Z^* plane for a single parallel RC element is a semi-

circle which passes through the origin and gives a low frequency intersection on the real axis corresponding to the resistance of the element. Note that in a polycrystalline sample, the equivalent circuit is formed by parallel RC circuits in series. In this way grain and grain boundary contributions are taken into account. As complex permittivity and complex impedance are related through $Z^* = 1/Y^* = 1/(j\omega C_0 \varepsilon^*)$, a relaxation in Z space (Fig. 4.6) can be transformed into a permittivity frequency spectrum.

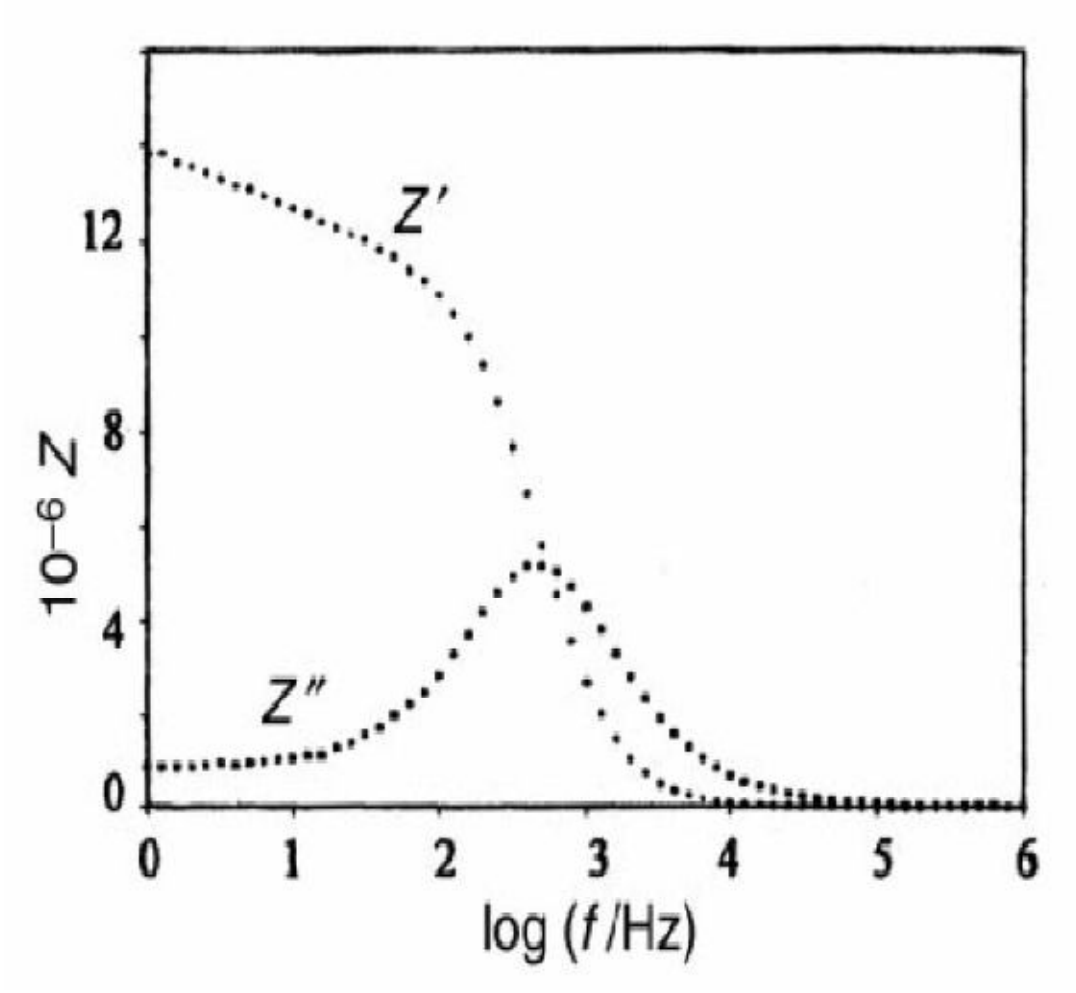

Figure 4.6: Frequency dependence of Z' and Z"

Real and imaginary parts of ε^* can be affected by the conduction, especially in the low frequency range. An increase in both ε' and ε'' is observed when the frequency decreases. No loss peak appears when the ionic conductivity dominates the dielectric response. Experimental data can also be analyzed in complex modulus formalism, $M^*=1/\varepsilon^*=j(\omega C_0)Z^*$, which allows a reduction of the grain boundary contribution. The relaxation frequency can be determined by plotting M''/M''_{max} as a function of frequency (M'' is the imaginary part of the complex modulus; M''_{max} is the maximum value). Impedance spectroscopy is particularly suitable for reflecting

microstructural features in ceramics since it allows the separation of bulk and grain boundary contributions.

In the current study the dielectric constant and loss tangent was calculated directly form the values of the capacitance measured using HP 4192A impedance bridge. The capacitance was measured at different temperatures and frequencies. Since the allowed frequency of the bridge was only 10 MHz which is in fact a useful range for the material to be used in devices. Also temperature range was kept between the room temperature and the T_C. The schematic diagram of the set up used for measuring the dielectric constant (Sample holder with temperature controller) is given in the figure 4.7.

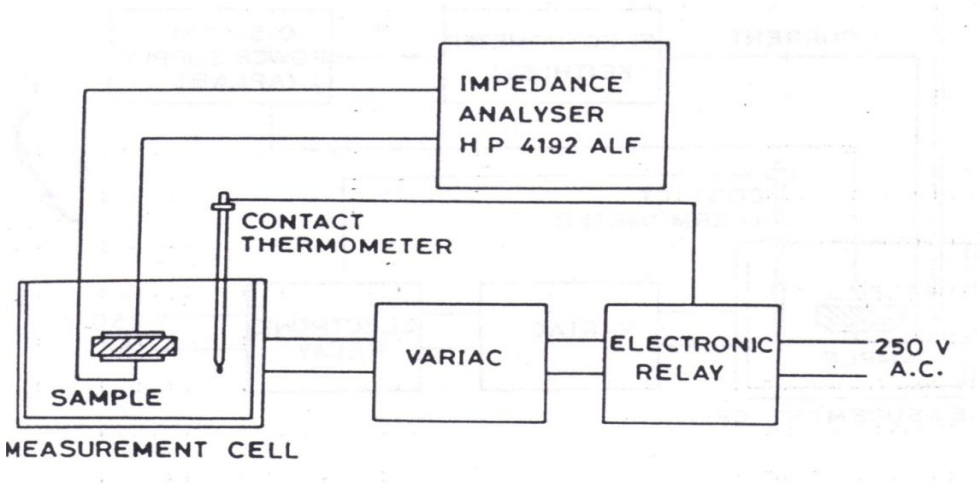

Figure 4.7: The schematic diagram of the set up used for measuring the dielectric constant

4.4.4 Conductivity Studies:

The conductivity of the sample was studied at different temperature. For the study a high voltage power supply (Aplab 5kV max) was used in series with the sample and electrometer. The current so obtained (I) was converted to current density (j) and the voltage applied (V) into the Field (E), by knowing the electrode area and thickness of the sample. The set up used similar as in figure 4.8. Now the voltage supply is also

added in series with the electrometer. To find the activation energies and the mechanism of conductivity in the sample, the conductivities are plotted against the reciprocal of the logarithm of the temperature in absolute scale [107]. Here the energies (E_a) can be calculated. Since the conductivity follow the relation mentioned below.

$$\sigma = \sigma_o \exp(-E_a/kT) \qquad \text{---------- (4.7)}$$

which implies

$$\ln \sigma = \ln \sigma_o - E_a/kT \qquad \text{---------- (4.8)}$$

Therefore a linear relation exists between ln σ and 1/T whose slope is $-E_a$.

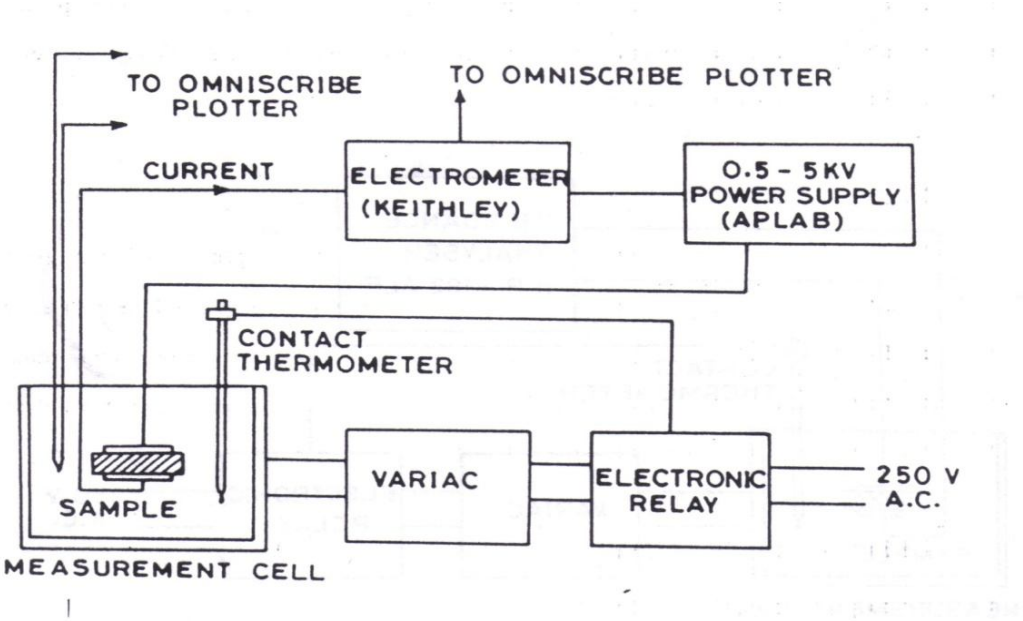

Figure 4.8: A set up to study conductivity of the samples.

4.5 Summary:

In this chapter Introduction, the oxide route method for preparing CCTO, preparation of CCTO-PVC composites, characterization of CCTO and CCTO-PVC composites have been described. The study continued in chapter-5 Analysis and Interpretation of data.